Effects of Aggregation and Mesomorphic Order on the Photophysical Properties of 4-Alkyl-*N*-(*p*-cyanophenyl)piperidines. Molecules Capable of Forming Intramolecular Charge Transfer States[1]

Bashir M. Sheikh-Ali and Richard G. Weiss*

Contribution from the Department of Chemistry, Georgetown University, Washington, D.C. 20057

Received February 7, 1994®

Abstract: The photophysical properties of 4-alkyl-*N*-(*p*-cyanophenyl)piperidines (I) in dilute and concentrated solutions and in neat melt and nematic phases have been studied by means of their static absorption and fluorescence spectra and by picosecond time-domain emission measurements. Molecules of I contain a chromophore which is capable of forming intramolecular charge-transfer (ICT) excited states. Dilute solutions of I in polar solvents exhibit dual emission similar to that of *p*-(*N*,*N*-dimethylamino)benzonitrile (DMABN). Evidence for several ground- and excited-state species, including two distinct complexes and a charge-transfer excited state of I, has been obtained in concentrated hexane solutions as well as in the neat liquid-crystalline and melt phases of I. In the time domain experiments on nematic and melt phases of a 1/1 (wt/wt) mixture of the pentyl and heptyl homologues of I, fluorescence from excitation at the red edge of the lowest energy absorption band rises "instantaneously" and the decay can be fit to a triple exponential function. The corresponding time-resolved emission spectra exhibit a time-dependent Stokes shift due to relaxation about a charge-transfer dominated excited-state species. In contrast, excitation near the lowest energy absorption maximum leads to fluorescence with a measurable rise time when emission is monitored at the long wavelength side of the emission band and an "instantaneous" rise when monitored at the short wavelength side of the band. A kinetic model consistent with these observations is proposed. It is shown that energy hopping from the excited singlet of I or its complexes is not an important contributor to the population of the charge-transfer species.

Introduction

Since the discovery of the dual fluorescence of (*N*,*N*-dimethylamino)benzonitrile (DMABN) in polar solvents,[2] a large number of publications has been devoted to the photophysical properties of DMABN and related molecules in the gas phase,[3] supersonic jets,[4] supercritcal fluids at different pressures,[5] polar and nonpolar low molecular weight solvents,[6–12] and polymer matrices.[13] The vast majority of these have dealt with very dilute solutions or conditions under which solutes are isolated from (and not oriented with respect to) each other.

Liquid-crystalline media are capable of orienting solutes and of affording important spectroscopic and mechanistic[14] information concerning their intermolecular interactions. For example, Sonnenschein and Weiss[15] observed that the fluorescence decays of α,ω-bis(1-pyrenyl)alkanes in cholesteric liquid-crystalline phases are monoexponential, but are multiexponential in non-viscous isotropic solvents. The simplification of the excimer kinetics in mesophases was explained in terms of limitations on the number of chain bending modes in the ordered phases. Sisido and co-workers[16] studied the kinetics of excimer formation of pyrenyl groups appended to cholesteryl esters in cholesteric phases. The greater restriction to reorientational motions of these pyrenyl groups was used to explain why their rate of excimer formation is smaller than that of pyrene dispersed in cholesteric liquid-crystalline solvents.[17] Recently, photophysical investigations of lumophores in neat liquid-crystalline phases formed from alkylcyanobiphenyls[18–20] (*n*-CB, where *n* = number of carbon atoms in the alkyl chain) and alkoxycyanobiphenyls[21] (*n*-OCB) have been conducted: crystalline 12-CB[19] exhibits both monomer

* Abstract published in *Advance ACS Abstracts*, June 1, 1994.

(1) Part 53 of our series "Liquid-crystalline Solvents as Mechanistic Probes". For part 52, see: Sheikh-Ali, B. M.; Weiss, R. G. *Liq. Cryst.* **1994**, in press.

(2) Lippert, E.; Lüder, W.; Boos, H. In *Advances in Molecular Spectroscopy*; Mangini, A., Ed.; Pergamon: Oxford, 1962; p 443.

(3) Peng, L. W.; Dantus, M.; Zewail, A. H.; Kemnitz, K.; Hicks, J. M.; Eisenthal, K. B. *J. Phys. Chem.* **1987**, *91*, 6162.

(4) (a) Warren, J. A.; Bernstein, E. R.; Seeman, J. I.; *J. Chem. Phys.* **1988**, *88*, 871. (b) August, J.; Palmer, T. F.; Simons, J. P.; Jouvet, C.; Rettig, W. *Chem. Phys. Lett.* **1988**, *145*, 273. (c) Kobayashi, T.; Futakami, F.; Kajimoto, O. *Chem. Phys. Lett.* **1987**, *141*, 450.

(5) Kajimoto, O.; Futakami, F.; Kobayashi, T.; Yamasaki, K. *J. Phys. Chem.* **1988**, *92*, 1347.

(6) Rotkiewicz, K.; Grellmann, K. H.; Grabowski, Z. R. *Chem. Phys. Lett.* **1973**, *19*, 315.

(7) Lippert, E.; Rettig, W.; Bonacic-Koutecky, V.; Heisel, F.; Miehé, J. A. In *Advances in Chemical Physics;* Prigogine, I., Rice, S. A., Eds.; John Wiley & Sons: New York, 1987.

(8) (a) Lippert, E. *Ber. Bunsenges. Phys. Chem.* **1988**, *92*, 417. (b) Zander, M.; Rettig, W. *Chem. Phys. Lett.* **1984**, *110*, 602.

(9) (a) Rotkiewicz, K.; Rubaszewska, W. *J. Lumin.* **1982**, *27*, 221. (b) Rotkiewicz, K.; Rubaszweska, W. *J. Lumin.* **1984**, *29*, 329. (c) Rotkiewicz, K.; Grabowski, Z. R.; Krowczynski, A.; Kühnle, W. *J. Lumin.* **1976**, *12/13*, 877.

(10) Rotkiewicz, K.; Rubaszewska, W. *Chem. Phys. Lett.* **1980**, *70*, 444.

(11) Heisel, F.; Miehé, J. A.; Martinho, J. M. G. *Chem. Phys.* **1985**, *98*, 243.

(12) (a) Hicks, J. M.; Vandersall, M. T.; Sitzmann, E. V.; Eisenthal, K. B. *Chem. Phys. Lett.* **1987**, *135*, 413. (b) Hicks, J. M.; Vandersall, M.; Babarogic, Z.; Eisenthal, K. B. *Chem. Phys. Lett.* **1985**, *116*, 18.

(13) (a) Al-Hassan, K. A.; Azumi, T. *Chem. Phys. Lett.* **1989**, *163*, 129. (b) Bokobza, L.; Cazeau-Dubroca, C.; Nouchi, G.; Ben Brahim, M.; Cazeau, P. *Polym. Bull.* **1992**, *28*, 709.

(14) (a) Weiss, R. G.; Ramamurthy, V.; Hammond, G. S. *Acc. Chem. Res.* **1993**, *26*, 531. (b) Ramamurthy, V.; Weiss, R. G.; Hammond, G. S. In *Advances in Photochemistry;* Volman, D. H., Hammond, G. S., Neckers, D. C., Eds.; John Wiley & Sons: New York, 1993; Vol. 18, p 67. (c) Weiss, R. G. In *Photochemistry in Organized and Constrained Media;* Ramamurthy, V., Ed.; VCH: New York, 1991; Chapter 14. (d) Khetrapal, C. L.; Weiss, R. G.; Kunwar, A. C. In *Liquid Crystals—Applications and Uses;* Bahadur, B., Ed.; World Scientific: Teaneck, NJ, 1990; Vol. II, Chapter 5. (e) Weiss, R. G. *Tetrahedron* **1988**, *44*, 3413. (f) Kalyanasundram, K. *Photochemistry in Microheterogeneous Systems*; Academic: Orlando, 1987.

(15) Sonnenschein, M. F.; Weiss, R. G. *J. Phys. Chem.* **1988**, *92*, 6828.

(16) Sisido, M.; Wang, X.; Kawaguchi, K.; Imanishi, Y. *J. Phys. Chem.* **1988**, *92*, 4797.

(17) Anderson, V. C.; Weiss, R. G. *J. Am. Chem. Soc.* **1984**, *106*, 6628.

(18) (a) Markovitsi, D.; Ide, J. P. *J. Chim. Phys.* **1986**, *83*, 97. (b) Baeyens-Volant, D.; David, C. *Mol. Cryst. Liq. Cryst.* **1985**, *116*, 217.

(19) Subramanian, R.; Patterson, L. K.; Levanon, H. *Chem. Phys. Lett.* **1982**, *93*, 578.

(20) Ikeda, T.; Kurihara, S.; Tazuke, S. *J. Phys. Chem.* **1990**, *94*, 6550.

(21) Tamai, N.; Yamazaki, I.; Masuhara, H.; Mataga, N. *Chem. Phys. Lett.* **1982**, *104*, 485.

and excimer bands; crystalline 7-CB,[18] 8-CB,[18] 3-OCB,[22] and 8-OCB[21] exhibit only monomer emission; in the liquid-crystalline and melt phases, both monomer and excimer emissions were observed in all cases. Also, the emission properties of columnar discotic liquid-crystalline phases comprised of molecules with phthalocyanine or triphenylene lumophores have been studied by steady-state and time-resolved spectroscopies.[23] It has been shown that exciton migration within the columnar phase of triphenylenes can be discribed as a one-dimensional random walk.[23a]

However, we are not aware of any reports on the photophysical behavior of neat or doped mesophases of molecules like DMABN capable of forming intramolecular charge-transfer (ICT) excited states. To this end, we have investigated the static and dynamic spectroscopic properties of dilute and concentrated solutions of 4-alkyl-*N*-(*p*-cyanophenyl)piperidines (I (n = 4–9)) and of the neat nematic and melt phases of a 1/1 (wt/wt) mixture of I (n = 5) and I (n = 7) (designated as I-57). These studies provide insights into the competition between the various unimolecular excited state processes which are known to occur and the bimolecular ones which are not well-documented. The results in the concentrated solutions and neat phases of I support the presence of at least two excited-state complexes, one of which originates from ground state complexes and the other which does so only partially. A detailed scheme is presented to explain the complex static and dynamic behavior.

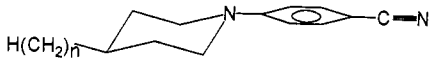

Experimental Section

The syntheses of I and characterization of the nematic phases formed by their mixtures have been reported elsewhere.[24] Individual components were >99% pure by gas chromatographic analysis. I-57 has a relatively stable monotropic nematic phase below 18.6 °C.[24] Absorption spectra were obtained with a Perkin-Elmer Lambda 6 spectrophotometer (1 nm slits) using 1 cm or 0.1 mm quartz cuvettes. Spectra from nematic and isotropic I-57 were obtained from a thin film of the material sandwiched between two quartz plates and thermostated at the desired temperature. Stationary state excitation and emission spectra were recorded on a Spex Fluorolog 2 spectrofluorometer (150 W Osram XBO xenon lamp; 1 nm slits) interfaced with an IBM-386 compatible computer. The wavelength-dependence of the lamp was corrected for the excitation spectra by using a solution of 3 g L^{-1} rhodamine B in ethylene glycol as a quantum counter.[25] Solutions of $\leq 10^{-3}$ M I in hexane or acetonitrile and the I-57 samples were flame-sealed after being degassed by at least four freeze-pump-thaw cycles at $<10^{-3}$ torr. More concentrated solutions of I were saturated with nitrogen by bubbling. Emission from solutions of I with o.d. > 0.1 and from melt and nematic I-57 were monitored at the front face. Stationary state spectra of I-57 were obtained from samples immersed at the desired temperature for 10 min in a doubly-distilled high-boiling alkane (usually hexadecane) which was thermostated by a circulating water/ethylene glycol system. The bath temperature was constant within the precision limit of our thermocouple (0.3 °C). Hexane (Baker, spectral grade) and acetonitrile (Baker, analytical grade) were from freshly opened bottles.

Time-resolved measurements were performed with the picosecond time-correlated single-photon counting (TCSPC) system at the Regional Laser and Biotechnology Laboratories (RLBL) of the University of Pennsylvania.[26] The excitation source is a cavity-dumped dye laser (frequency doubled by a KDP crystal) synchronously pumped by a mode-locked Nd-YAG laser. Emitted light was passed through a polarizer at the "magic angle" and a monochromator and was detected by a microchannel plate photomultiplier tube (Hammamatsu R 2809U-07 MCP-PMT).

Histograms accumulated versus time were stored in a Nucleus PC-II multichannel analyzer. The instrument response functions, which have 75 ps full-width at half-maximum (FWHM), were used in the data analysis (deconvolution by iterative convolution nonlinear least-square method[27-29]). The number of exponential functions was incremented from one until an acceptable fit (as judged by the values of the reduced χ^2,[30] the Durbin–Watson parameter,[31] the randomness of the residuals[27] and the autocorrelation function[28]) was obtained. Values of reduced χ^2 and Durbin-Watson parameters for "acceptable" fits are listed in supplementary Tables 1–4; values of χ^2 between 0.91 and 1.34 and of the Durbin–Watson parameter between 1.51 and 2.09 were found for the reported fits.

Results and Discussion

A. Steady-State Measurements.

Isotropic Solutions. The nature of the fluorescence spectra of I in solution depends strongly on the solvent but not upon the chain length (n). Each of the homologues of I provided indistinguishable electronic absorption and emission spectra in isotropic media. With increasing solvent polarity, both the fluorescence and absorption spectra are shifted to longer wavelengths, but the emission is affected to a much greater extent. For example, emission maxima from 10^{-5} M I (n = 4) occur at 350 nm in hexane and at 355 and 475 nm in acetonitrile. The absorption and steady-state emission spectra of I are similar to those of DMABN.[9] Emission maxima at 340 and 475 nm have been assigned to transitions from a locally excited (LE) and a "twisted intramolecular charge transfer"[6,32] (TICT) state, respectively. Schuddeboom and co-workers[33] have proposed that the 475 nm band is from an intramolecular charge-transfer (ICT) state which need not be in a twisted conformation. Cazeau-Dubroca and co-workers[34] have attributed the longer wavelength emission from DMABN in polar aprotic solvents to excited states formed from pretwisted ground-state molecules which are complexed to water, present as a trace impurity.[34] Regardless of their origin, the absorption and excitation spectra of dilute solutions of I are very similar (λ_{max} = 286 nm in hexane and 297 nm in acetonitrile). The temporal decay of the longer-wavelength emission (λ_{ex} 310 nm) can be fit satisfactorily to a single exponential function whose decay constant Λ, 3.6 ± 0.1 ns (χ^2 = 1.1), is near that of the longer wavelength emission from DMABN in polar, low viscosity solvents.[35] Since the ratio of the intensities of the emission bands from I in acetonitrile is excitation wavelength dependent, the two excited states responsible are not equilibrated during their lifetimes and must be formed from distinct ground-state species.

Figure 1 shows the excitation wavelength dependence of the emission spectra of a 0.11 M solution of I (n = 7) in hexane. They indicate the presence of more than one species: at λ_{ex} 280–320 nm, the major emission is centered at 380 nm; when λ_{ex} is 340–

(22) (a) David, C.; Baeyens-Volant, D. *Mol. Cryst. Liq. Cryst.* **1984**, *106*, 45. (b) David, C.; Baeyens-Volant, D. *Mol. Cryst. Liq. Cryst.* **1989**, *168*, 37.

(23) (a) Markovitsi, D.; Lecuyer, I.; Lianos, P.; Malthete, J. *J. Chem. Soc. Faraday Trans.* **1991**, *87*, 1785. (b) Markovitsi, D.; Bengs, H.; Ringsdorf, H. *J. Chem. Soc. Faraday Trans.* **1992**, *88*, 1275. (c) Markovitsi, D.; Lecuyer, I.; Simon, J. *J. Phys. Chem.* **1991**, *95*, 3620.

(24) (a) Sheikh-Ali, B. M.; Weiss, R. G. *Liq. Cryst.* **1991**, *10*, 575. (b) Sheikh-Ali, B. M.; Weiss, R. G. *Liq. Cryst.*, in press.

(25) (a) Karstens, T.; Kobs, K. *J. Phys. Chem.* **1980**, *84*, 1871. (b) Mekhush, W. H.; *Appl. Opt.* **1975**, *14*, 26.

(26) Holtom, G. R. In *Time-Resolved Laser Spectroscopy in Biochemistry II;* Proceedings of the SPIE (15–17 Jan, 1990, Los Angles), Vol. 1204, SPIE: Bellingahm, 1990.

(27) O'Connor, D. V.; Phillips, D. *Time-Correlated Single Photon Counting*; Academic: New York, 1984.

(28) Demas, J. N. *Excited State Lifetime Measurements;* Academic: New York, 1983.

(29) (a) Hall, P.; Selinger, B. *J. Phys. Chem.* **1981**, *85*, 2941. (b) Daniels, R. W. *An Introduction to Numerical Methods and Optimization Techniques;* North-Holland: Amsterdam, 1978.

(30) (a) Grinvald, A.; Steinberg, I. Z. *Anal. Biochem.* **1974**, *59*, 583. (b) Bevington, P. R. *Data Reduction and Error Analysis for the Physical Sciences;* McGraw-Hill: New York, 1969.

(31) Durbin, J.; Watson, G. S. *Biometrika* **1951**, *38*, 159.

(32) Rettig, W. *J. Lumin.* **1980**, *26*, 21.

(33) Schuddeboom, W.; Jonker, S. A.; Warman, J. M.; Leinhos, U.; Kühnle, W.; Zachariasse, K. A. *J. Phys. Chem.* **1992**, *96*, 10809.

(34) Cazeau-Dubroca, C.; Ait Lyazidi, S.; Cambou, P.; Peirigua, A.; Cazeau, Ph.; Pesquer, M. *J. Phys. Chem.* **1989**, *93*, 2347.

(35) Rotkiewicz, K.; Köhler, G. *J. Lumin.* **1987**, *37*, 219.

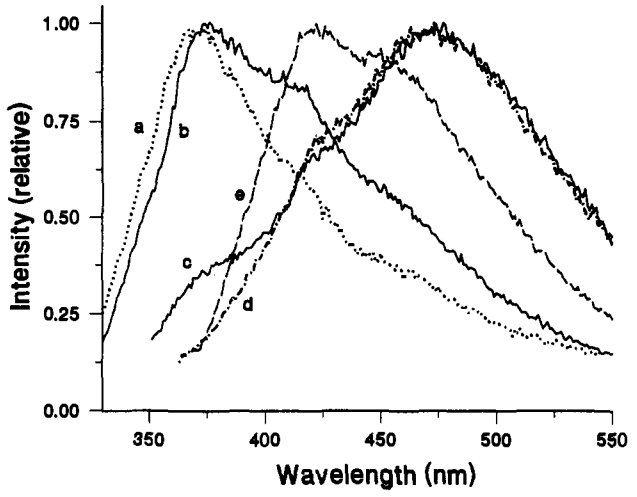

Figure 1. Emission spectra of 0.11 M I (n = 7) in hexane excited at (a) 280, (b) 300–320 (c) 340, (d) 350, and (e) 360 nm.

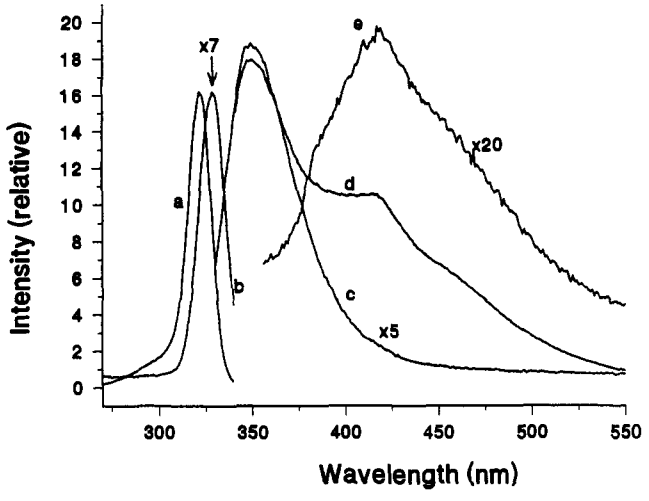

Figure 2. Excitation spectra (corrected) of 4 × 10^{-3} M I (n = 4) in hexane monitored at (a) 350 and (b) 460 nm and emission spectra excited at (c) 300, (d) 330, and (e) 345 nm.

350 nm, a weaker emission near 420 and a stronger one near 460 nm are evident; at λ_{ex} 360 nm, the 420 and 460 nm emissions are dominant. The variation of the 380, 420, and 460 nm intensity ratios with excitation wavelength again indicates the presence of different species which do not equilibrate completely during their excited-state lifetimes. The 380 nm band can be ascribed to emission from unassociated molecules of I; since the 420 and 460 nm bands do not appear in very dilute solutions, they must emanate from complexes which are either present in the ground state[36] or which form after excitation.

The emission band at 420 nm was also observed in the spectrum of 4 × 10^{-3} M I in hexane at λ_{ex} > 330 nm. Under these conditions, the 460 nm band, if present at all, is a weak shoulder (Figure 2) and the highest energy emission band (355 nm) emanates from an LE state of unassociated I. Since the 355 and 420 nm emissions can be produced selectively by different excitation wavelengths, the species responsible for them are not different.

In spite of the complexity of the emission spectra from >10^{-4}M I in hexane, absorption spectra of ≤10^{-2} M I do not provide evidence for ground-state aggregation. However, excitation spectra of 4 × 10^{-3} M and 0.11 M I in hexane are strongly dependent on the emission wavelength. For 0.11 M I at emission wavelengths <400 nm, the excitation spectra consist of a strong

(36) (a) Nakashima, N.; Mataga, N. *Bul. Chem. Soc. Jpn.* **1973**, *46*, 3016. (b) Nakashima, N.; Inoue, H.; Mataga, N.; Yamanaka, C. *Bul. Chem. Soc. Jpn.* **1973**, *46*, 2288.

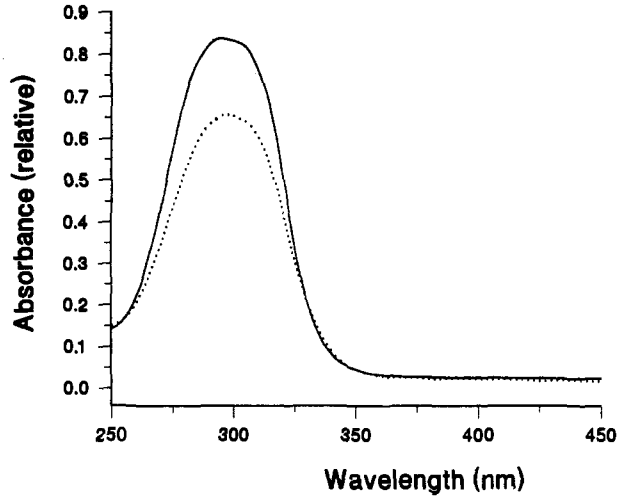

Figure 3. Absorption spectra of I-57 (obtained from a thin film of sample sandwiched between two quartz plates) at (···) 15 °C, nematic phase, and (—) 25 °C, melt phase.

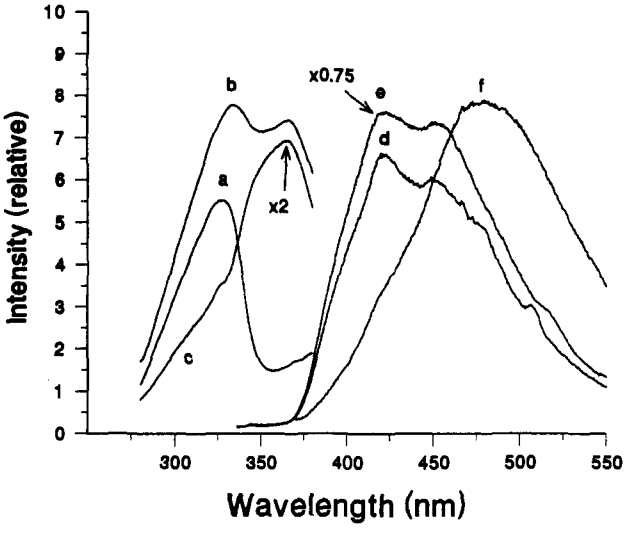

Figure 4. Excitation spectra (corrected) of I-57 at 15 °C (nematic phase) monitored at (a) 400, (b) 470, and (c) 550 nm, and emission spectra excited at (d) 300, (e) 325, and (f) 360 nm.

broad band at ca. 300 nm and a weaker one at 365 nm. As λ_{em} is increased, the intensities of the 365 and 300 nm bands increase and decrease, respectively, until at λ_{em} 450 nm, only the 365 nm band can be detected. Further increases of λ_{em} results in excitation spectra which are broadened and hypsochromically shifted; the excitation maximum is 345 nm when the λ_{em} is 550 nm.

Liquid-Crystalline and Melt I-57. Excitation and emission spectra of the I-57 mixture in its nematic phase have features which are somewhat similar to those of concentrated I in nonpolar solvents (i.e., where molecular aggregation is favored). Absorption spectra of nematic and isotropic (melt) I-57 are broad and have maxima at ca. 297 nm (Figure 3). The emission and excitation spectra at 15 °C (nematic phase) exhibit a strong wavelength dependence (Figure 4). Excitation wavelengths <340 nm result in emissions dominated by two overlapping bands at about 420 and 460 nm. As λ_{ex} is increased, the two bands decrease while a new one grows at 480 nm until at λ_{ex} 360 nm, only the 480 nm band has appreciable intensity.

When emission is monitored at <420 nm, the excitation spectrum of the nematic phase is centered at 325 nm. As λ_{em} is increased, the excitation spectrum broadens and a new band grows at 360 nm. It dominates the spectrum when λ_{em} is >500 nm. The emission spectra of I-57 in its melt phase at 25 °C are similar to those of the nematic phase except that the 460 nm band is less

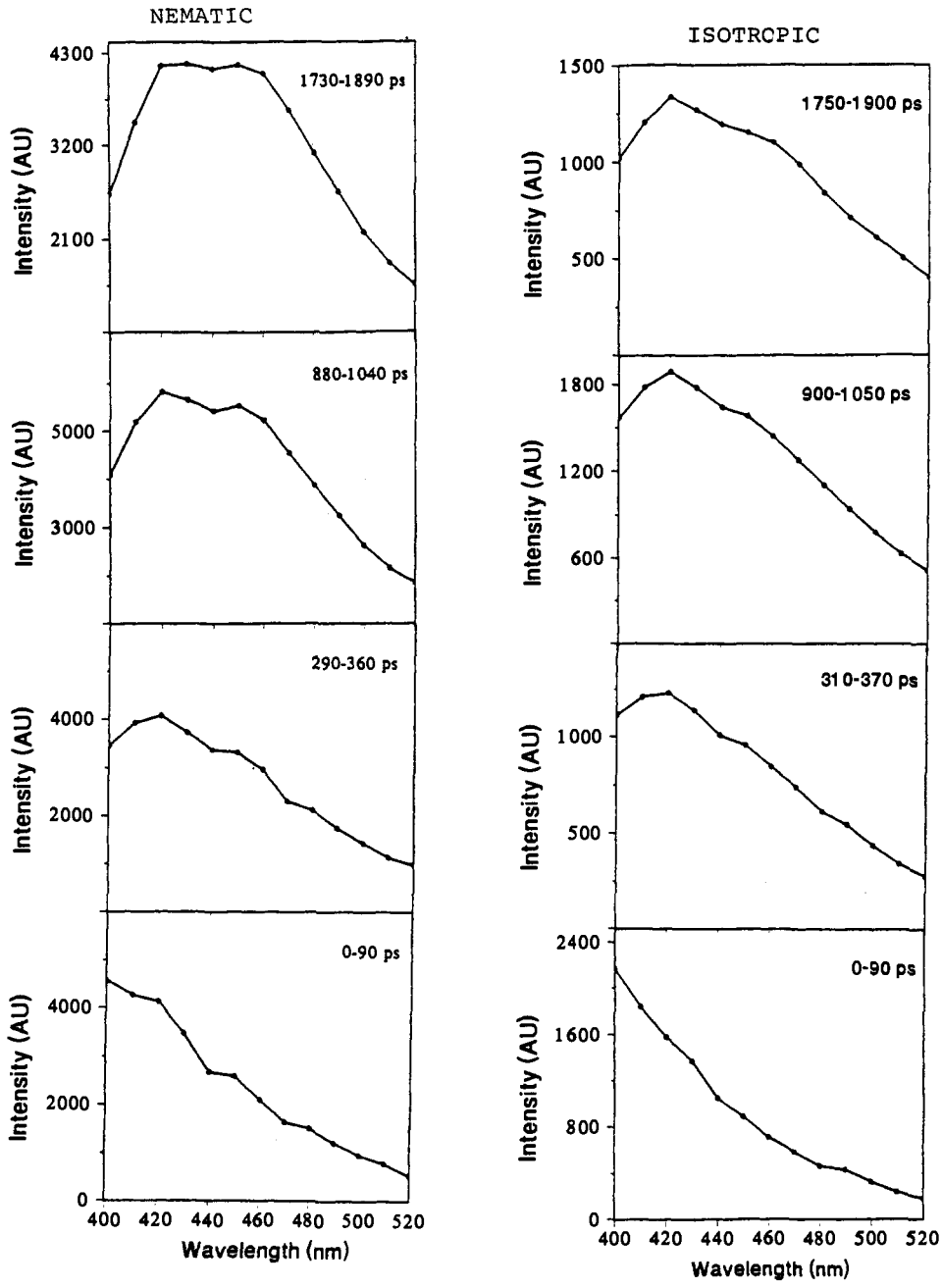

Figure 5. Time-resolved fluorescence spectra of I-57 at 15 °C (nematic phase) and 25 °C (melt phase) calculated as described in the text. The excitation wavelength is 325 nm. Time-windows are shown in each spectrum.

pronounced and there is a weak shoulder below 400 nm (presumably due to a monomeric emission like that at 380 nm observed in concentrated hexane solutions of I). The similarities of the emission spectra in neat nematic and melt phases of I-57 and in $>4 \times 10^{-3}$ M I in hexane indicate that similar nonequilibrated excited-state species (but in different relative populations) are present.

B. Transient Measurements.

In order to characterize further the natures of the emitting species in the neat nematic and melt phases of I-57, fluorescence decay characteristics in the picosecond–nanosecond time regime were studied. Excitation wavelengths of 325 and 360 nm (representing the blue and red sides of the lowest energy band in the excitation spectrum) and emission wavelengths from 400–520 nm in 10 nm increments were interrogated. Each decay was analyzed using weighted nonlinear least-square (NLLS) deconvolution methods.

Time-resolved fluorescence (TRF) spectra were calculated from sets of decay curves obtained under identical conditions at each excitation wavelength except for the monitoring wavelength. The fraction of light emitted during a "time window" can be normalized to the intensity of a stationary state fluorescence spectrum according to eqs 1 and 2.[27]

$$G^{\circ}(\lambda_j, t_2 - t_1) = \frac{G(\lambda_j, t_2 - t_1)F(\lambda_j)}{\int_0^{\infty} G(\lambda_j,t)\,dt} \quad (1)$$

$$G(\lambda_j, t_2 - t_1) = \int_{t_1}^{t_2} G(\lambda_j,t)\,dt \quad (2)$$

In these equations, $t = t_2 - t_1$ is the time-window of interest, $G(\lambda_j,t)$ is the decay function monitored at wavelength λ_j, $F(\lambda_j)$ is the steady state fluorescence intensity at λ_j, and

$$\int_0^{\infty} G(\lambda_j,t)\,dt$$

is the total area under the decay curve. The ratio

$$\frac{G(\lambda_j, t_2 - t_1)}{\int_0^\infty G(\lambda_j, t)\, dt}$$

is the fraction of the total amount of light which is emitted in the $t_2 - t_1$ window.

For the calculation of the TRF spectra, decays were not deconvoluted from the instrument response function and the peak channel of the instrument response function was chosen as t = 0. By integrating over time windows instead of "one" particular time for the calculation of the TRF spectra, the decays are not forced to follow a particular function. The TRF spectra of I-57 in the nematic (15 °C) and melt (25 °C) phases (from excitation at one wavelength) are qualitatively similar. However, excitation at 325 and 360 nm gave very different TRF spectra. Thus, they will be treated separately.

325 nm Excitation. The early-time TRF spectra have maxima at wavelengths shorter than 400 nm in both the isotropic (melt) and nematic phases (Figure 5). Within about 200–300 ps, a new maximum develops at about 420 nm. At less than 200 ps in the nematic phase, a second band near 460 nm begins to appear as a shoulder; in the melt phase, at least 600 ps are required for the corresponding shoulder to be evident (Figure 5). To develop fully, the shoulder requires about 600 ps in the nematic phase and more than 2 ns in the isotropic (melt) phase. The phase dependence on the growth time of the 460 nm shoulder suggests that it originates from emission of a dynamically formed complex (or complexes), $\mathbf{I_{2b}}^*$.

In the nematic phase of I-57, molecules are aligned with their long axes parallel on average. If the excited-state complexes are comprised of two parallel (or antiparallel) molecules, their formation should be faster in the nematic phase due to prealignment before excitation; in the melt phase, molecules are oriented rather randomly, and the time for formation of excited-state complexes will be slowed by the need to reorient vicinal pairs.

All fluorescence decay curves required a sum of at least two exponential functions to obtain acceptable fits. A typical accepted triple exponential fit for a decay curve and unacceptable fits using fewer exponential terms are shown in Figure 6. In the higher energy parts of the emission spectra of I-57 at 25 °C, short (100–200 ps), intermediate (0.6–0.8 ns), and longer (3.3–3.5 ns) decay constants with positive preexponentials were needed to obtain good fits; in the corresponding longer wavelength parts (λ>460 nm), 100–200 ps rise and 3.4–3.6 ns decay time constants were sufficient. The 100–200 ps rise in the lower energy region is probably linked to the 100–200 ps decay on the higher energy side; they relate to the rate of formation of $\mathbf{I_{2b}}^*$ from I* and I and the rate of loss of emission from I* due to its combination with molecules of I. Therefore, 3.4–3.6 ns is the lifetime of $\mathbf{I_{2b}}^*$ (*vide infra*).

Similar behavior is observed in the nematic phase. Although the decay constants of the longer-lived component in the nematic phase (3.7–4.2 ns) are slightly longer than those in the melt phase, the rise component on the red side and the shortest decay component on the blue side of the emission are similar in magnitude in the two phases. A third (decay) component, whose time constant is 0.6–1.1 ns in the melt phase and 0.4–0.8 ns in the nematic phase, can be attributed to a superposition of emissions from monomer ($\lambda_{max} \sim 380$ nm), excimer $\mathbf{I_{2b}}^*$ ($\lambda_{max} \sim 460$ nm), and a third species $\mathbf{I_{2a}}^*$ ($\lambda_{max} \sim 420$ nm).

The 420 nm emission in the melt and nematic phases of I-57 appears similar in shape, energy, and origin to the 420 nm emission band observed in $\geq 4 \times 10^{-3}$ M hexane solutions of I; the steady-state excitation and emission spectra indicate that the 420 nm band is *not* from excited-state monomer. Furthermore, the protracted rise in histograms monitored at >450 nm demonstrates

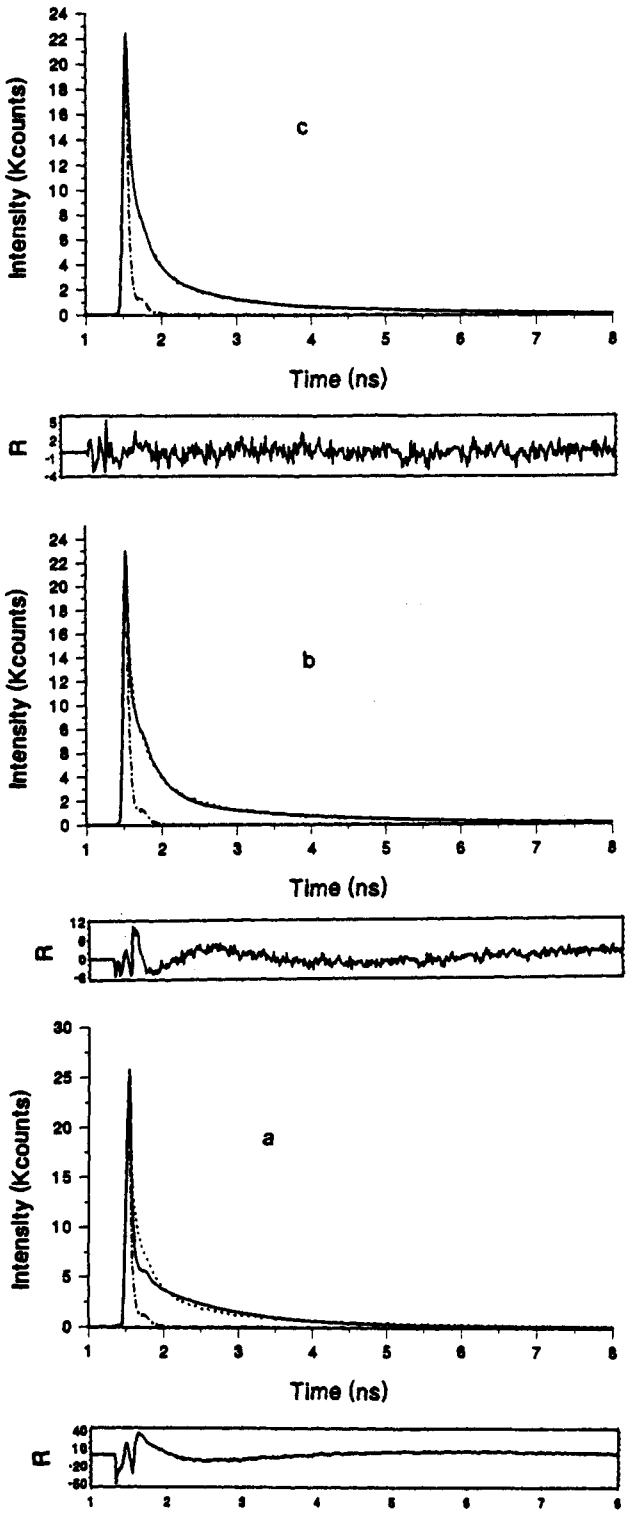

Figure 6. A typical fluorescence decay curve of I-57 (λ_{ex} = 360 nm; λ_{em} = 410 nm; T = 25 °C) and its best fit with residuals to (a) a single exponential function (τ = 1.1 ns; χ^2 = 73); (b) a double exponential function (τ_i = 2.2, 0.3 ns; χ^2 = 5.1); (c) a triple exponential function (τ_i = 2.8, 0.6, 0.1 ns; χ^2 = 1.4). The instrument response function is also shown.

that both static and dynamic processes must contribute to the formation of the species emitting at 460 nm.

It is also noteworthy that there is no detectable protracted rise component to the histogram of Figure 6. Since emission at 410 nm is due principally to I* and $\mathbf{I_{2a}}^*$, we conclude that the latter is formed almost exclusively upon excitation of ground-state complexes, $\mathbf{I_{2a}}$; there is no evidence for their formation in a dynamic process analogous to that responsible for some of the $\mathbf{I_{2b}}^*$. It is

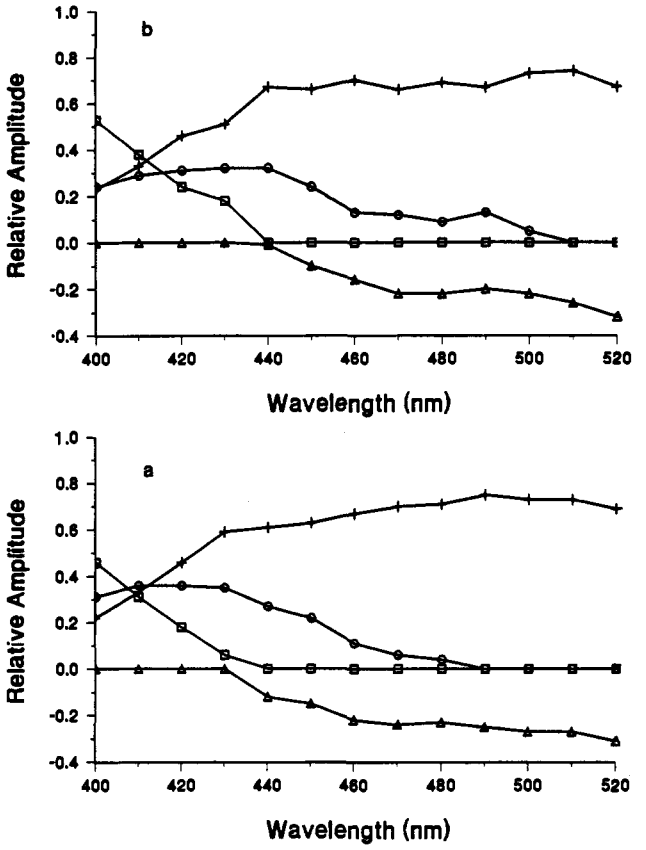

Figure 7. Plots of the relative amplitudes of the preexponentials obtained from the global analysis of the decay curves monitored at different wavelengths of the emission spectrum of I-57. (a) At 15 °C (nematic phase): (□) τ = 0.2 ns, decay; (△) τ = 0.2 ns, rise; (○) τ = 1.2 ns, decay; (+) τ = 3.9 ns, decay. (b) At 25 °C (melt phase): (□) τ = 0.1 ns, decay; (△) 0.2 ns, rise; (○) 0.8 ns, decay; (+) 3.5 ns, decay. Lines are intended to show trends between data points.

unknown whether the I_{2a}* and I_{2b}* are capable of dissociating to I* and I during their excited-state lifetimes. The ambiguity of this point is discussed later.

The set of decay curves with 325 nm excitation has been analyzed simultaneously using a NLLS global analysis method.[37] Figure 7 shows the relative amplitudes of the various decay components obtained from the global analysis of the decay curves of I-57 as a function of the monitoring wavelength. They were obtained by forcing the three decay constants of each set of histograms to be the same and allowing the preexponential factors to vary independently. From the nematic phase data set, a faster (0.2 ns) and a slower decay component (1.2 ns) in the higher energy part of the emission spectrum, a fast rise (0.2 ns) in the lower energy part, and a slow (3.9 ns) decay component throughout the 400–520 nm range were obtained. In the melt phase, the corresponding decay components have the following values: 0.1 and 0.8 ns (decay) in the higher energy part of the spectrum, a 0.2 ns rise in the lower energy region, and a 3.5 ns common decay.

Consistent with the analysis using the NLLS method, decay curves monitored at $\lambda_{em} \leq 450$ nm require a sum of three exponentials to obtain acceptable fits, while those monitored at ≥460 nm can be fit acceptably with only a rise and a decay term. It is reassuring that the magnitudes of the time constants from the NLLS and global analysis methods are also similar.

360 nm Excitation. The TRF spectra from I-57 irradiated at 360 nm (Figure 8) or at 325 nm (Figure 5) have very different shapes and time evolutions. Initially, there is a maximum at ca. 470 nm in the 360 nm excitation spectra which shifts with time to ca. 490 nm; this corresponds to a maximum time-dependent Stokes shift of 800–900 cm^{-1}. The TRF spectra from I-57 after the Stokes shift is complete (i.e., >400 ps in the melt phase and >500 ps in the nematic phase) resemble closely the stationary state emission spectra. Note that the Stokes shift requires a slightly longer period in the nematic phase. It is not an instrumental artifact related to the lack of response function deconvolution since it persists well beyond 75 ps and is absent from the TRF spectra calculated from 325 nm excitations.

Shorter (ca. 100 ps), intermediate (0.5–0.7 ns), and longer (2.2–2.5 ns) time constants with positive preexponentials were required to fit satisfactorily the decay curves in the nematic phase. For the melt phase, 100–200 ps, 0.6–1.2 ns, and 2–2.8 ns constants with positive preexponentials were calculated. The peak channels of all decay functions excited at 360 nm are within two channels (34 ps) of the maxima for the instrument response functions. This indicates an excited state(s) whose formation time is <75 ps, the limit of the instrument's resolution. The presence of the time-dependent Stokes shift suggests that the source of complexity in the emission decays is the relaxation of ground-state molecules around a highly polar excited-state molecule. Apparently, a charge-transfer (CT) state forms within the instrument response time from the excitation of (less-polar) ground-state I. The molecules of I comprising the "solvent" rearrange themselves to accommodate the excited polar species in their midst.

Su and Simon[38] have observed that the ICT emission from DMABN in alcohol solutions over the temperature range of –60 to 0 °C is also accompanied by a time-dependent Stokes shift. The emission decay was reported to be nonexponential at short times and to remain so to the longest relaxation time of the solvent. As in the case of I-57 excited at 360 nm, at least three exponential terms were needed to obtain an acceptable fit in the region where solvent relaxation is effective. At 360 nm excitation, it is possible that only a small fraction of the I-57 molecules, having an "appropriate" conformation to undergo an intramolecular charge-transfer transition within the time period of the instrument response, may be absorbing. The relatively long relaxation time in the nematic and melt phases, 400–500 ps, is consistent with the period expected for molecular motions of neighboring solvent molecules in a viscous medium like that offered by I-57. The slightly faster relaxation in the melt phase may be due to its lower viscosity and with greater availability of specific relaxation modes for solvent reorganization around the CT species.

C. A Kinetic Model.

We considered initially the possibility that energy migration (hopping) in I-57 from I* or I_2* (either a or b) to the ICT excited state A* (as a trap) may take place.[23] The fact that ICT emission is not observed for $\lambda_{ex} < 330$ nm suggests that such a mechanism does not occur. Regardless, an attempt has been made to reproduce the fluorescence decay $G(t)$ of the charge transfer state assuming multistep excitation–migration[39] using a "random walk" model (eq 3).[40] In this equation, τ_D is the fluorescence

$$G(t) = e^{t/\tau_D} e^{-\rho a (t/\tau_i)^{d/2+1}/2\rho^2 b (t/\tau_i)^d} \quad (3)$$

lifetime of the donor; τ_i is the average transfer time between monomers, $\rho = -\ln(1-p)$, p is the probability that the acceptors are randomly distributed, a and b are constants, and d is the spectral dimension. In this model,[40] the "walker" is trapped at the first possible opportunity. Although the equation yields acceptable fits for some decay curves, recovered parameters do not follow a consistent trend for different decay curves recorded at one temperature. This indicates that the hopping model is

(37) Knutson, J. R.; Beechem, J. M.; Brand, L. *Chem. Phys. Lett.* **1983**, *102*, 501.

(38) (a) Su, S.-G.; Simon, J. D. *J. Phys. Chem.* **1989**, *93*, 753. (b) Su, S.-G.; Simon, J. D. *J. Chem. Phys.* **1988**, *89*, 908.

(39) Takami, A.; Mataga, N. *J. Phys. Chem.* **1987**, *91*, 618.

(40) Klafter, J.; Blumen, A. *J. Chem. Phys.* **1984**, *80*, 875.

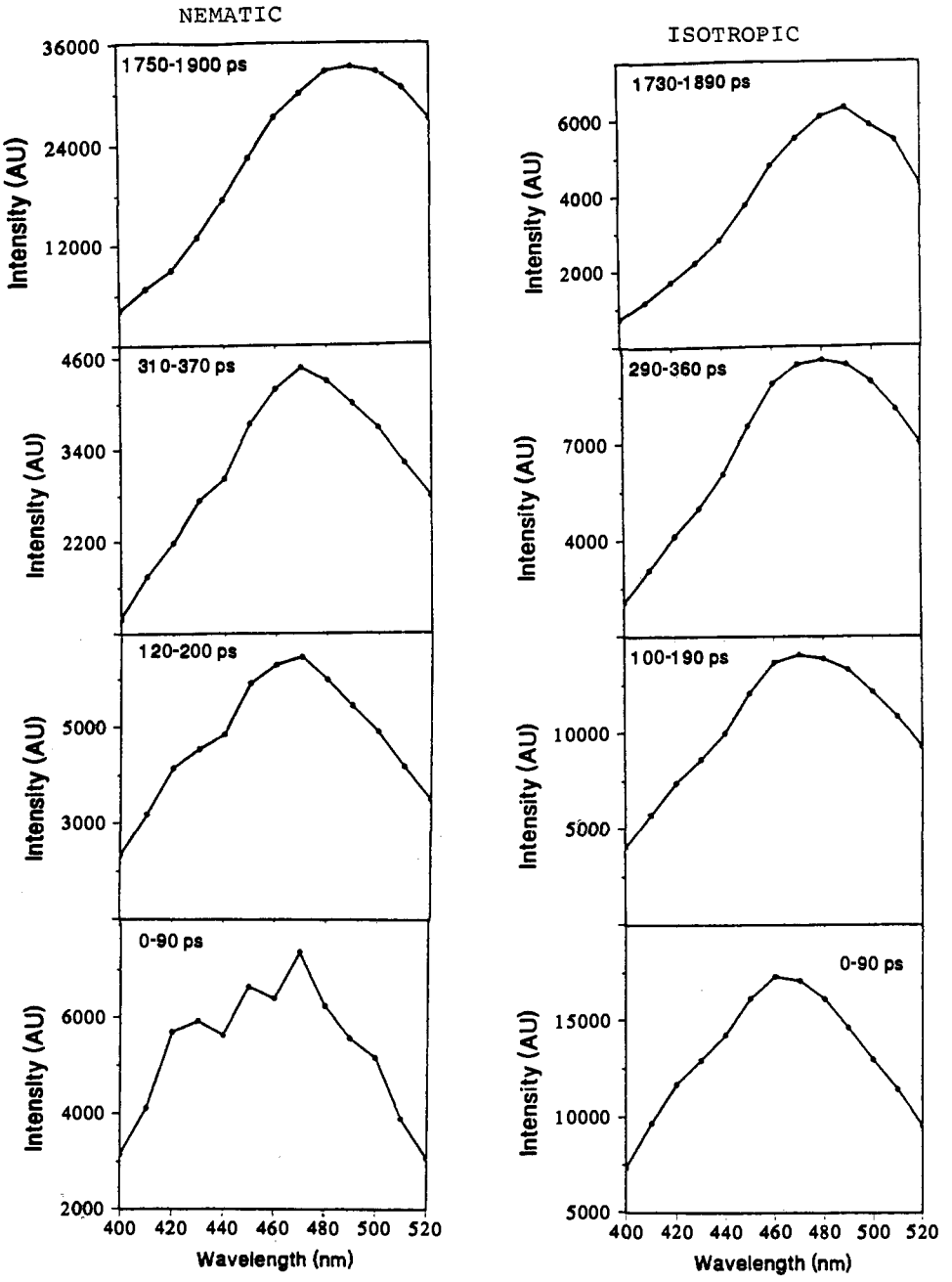

Figure 8. Time-resolved fluorescence spectra of I-57 at 15 °C (nematic phase) and 25 °C (melt phase) calculated as described in the text. The excitation wavelength is 360 nm. Time-windows are shown in each spectrum.

inappropriate for the present system; although eq 3 has a sufficient number of variables to allow individual curves to be fit well, comparisons demonstrate that its application is a mathematical exercise here, with no apparent physical meaning. For instance, at 25 °C and 360 nm excitation, τ_D = 9.5 ns, τ_i = 4.6 ns, and d = 0.39 (χ^2 = 1.5) are predicted when λ_{em} = 400 nm; but τ_D = 1.9 ns, τ_i = 0.5 ns, and d = 0.48 (χ^2 = 1.2) are calculated when λ_{em} = 520 nm.

The kinetic scheme proposed by Grabowski et al.[6] (Scheme 1) successfully explains the photophysical properties of very dilute solutions of DMABN in polar, low molecular weight solvents. It was assumed reasonably that solvent relaxation is much faster than the rate of intramolecular charge transfer, and that the anomalous emission originates from a charge-transfer species in a solvent-relaxed environment. The formation of excimers need not be considered since solute concentrations are low, excited-state lifetimes are short, and there is no evidence for ground-state aggregation; the experimental conditions are designed to avoid the complications this work seeks to study.

Since the 480 nm emission from the melt and nematic phases of I-57 is dominant only at excitation wavelengths >350 nm while the 420 and 460 nm bands are the principal ones at λ_{ex} < 340 nm, different photophysical processes must operate in different excitation regimes. Due to the charge-transfer character of the 480 nm band (N.B., the time-dependent Stokes shift), it will be discussed separately.

At excitation wavelengths <340 nm, I in various media has emission spectra which indicate the presence of at least three different excited-state species. Thus, a model more complex than that found in Scheme 1 must be invoked. The data presented thus far for I-57 are compatible with Scheme 2. It is a version of the model of Birks,[41] usually applied to the kinetics of excimer/exciplex formation,[42] but modified to consider the presence of ground-state complexes which attend the very high concentrations

(41) Birks, J. B.; Dyson, D. J.; Munro, I. H. *Proc. R. Soc.* **1963**, *275A*, 575.
(42) For instance, see: (a) Ware, W. R.; Watt, D.; Holmes, J. D. *J. Am. Chem. Soc.* **1974**, *96*, 7853. (b) Halpern, A. M.; Ravinet, P.; Sternfels, R. J. *J. Am. Chem. Soc.* **1977**, *99*, 169.

Scheme 1

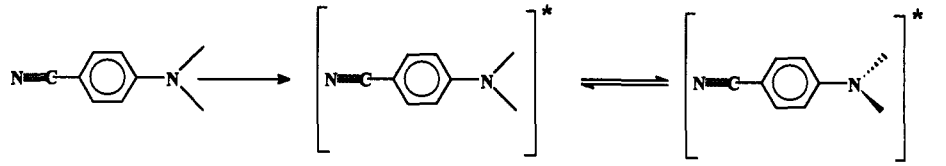

LE ICT

(Twisted conformation shown)

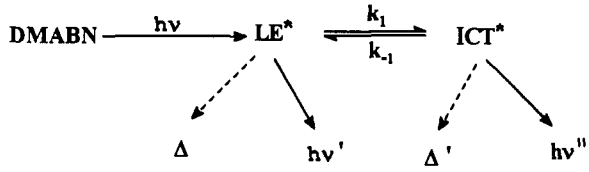

Scheme 2. Model for Photophysical Processes of I in I-57

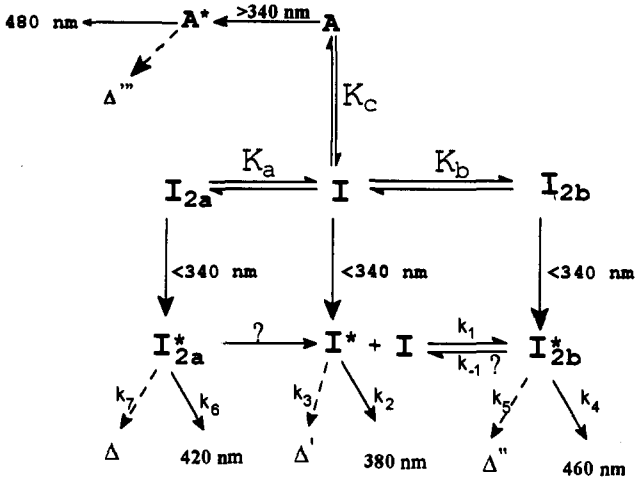

in a neat phase. Recently, Ikeda and co-workers[20] invoked the presence of analogous ground-state complexes to describe the photophysical properties of liquid-crystalline alkylcyanobiphenyls.

Our proposed model involves equilibration of a monomer (I) and two types of discrete ground state complexes (I_{2a} and I_{2b}), which are assumed to be dimeric. In fact, each of the complexes may include a family of structures and stoichiometries, related by the similarity of their spectral and temporal characteristics. For the purpose of simplicity, they will be treated as single entities. All of them can be excited by <340 nm radiation. The presence of a rise component in the histograms monitored at $\lambda_{em} > 450$ nm (Figure 6 and Supplementary Tables 1 and 2) indicates that a dynamically forming excited state complex from I* and I, leading to an "excimer" I_{2b}*, is involved, also.

The monomer emission is centered at ca. 380 nm. The emission maximum from I_{2a}* (the directly excited ground-state complex I_{2a}) appears at 420 nm and that from I_{2b}* at 460 nm. Whether dynamically formed I_{2b}* and that directly excited from the ground-state complex I_{2b} (statically formed) are equivalent (making the "excimer" notation inappropriate in the strict sense of the word) is unknown.

A mathematical solution to the kinetic model is included as an Appendix. It predicts a double exponential decay for both the monomer and the "excimer". This is the case when the excimer dissociation rate constant (k_{-1}), to give an excited state monomer, is an important kinetic pathway for deactivation. If $k_{-1} \sim 0$, $A_1 = X$, reducing α_2 to zero, and the monomer is predicted to decay exponentially. The observed triple exponential decay of histograms monitored around 400 nm and the similarity of the longest decay component on the lower and higher energy parts of the emission spectra of I-57 suggest a double exponential decay for the monomer. However, it is possible that emission from I_{2b}* appears in the 400–440 nm region of the spectrum.

Since the species emitting at ~460 nm can be populated directly, the preexponentials of the rise and decay components are not expected to (and do not) sum to zero. Also, these terms have non-zero amplitudes, α, at the maximum of the instrument response function. Thus, the relative amplitudes of the α_i at $t = 0$ depend on the concentrations and the extinction coefficients of the directly excited species. In turn, the relative populations of ground-state species depend on the values of the equilibrium constants, K_a and K_b. Although these constants are not known, both lower temperature and greater molecular ordering favor larger values in the nematic phase of I-57.

Why the monomeric (and presumably planar) I* species do not produce emissions characteristic of ICT states in nematic and isotropic I-57 is not clear. Viscosity[43] and polarity[12] are known to be important parameters which control ICT formation from a planar precursor. As mentioned previously, Schuddeboom and co-workers[33] argue that rotation around an amino-phenyl bond is *not* necessary for the formation of ICT excited states. It is quite possible in I-57 that any (planar) I* is quenched via complexation faster than it can twist or undergo any other conformational change which leads to a charge transfer state, A*. Regardless of the reason, there is no evidence to support the direct transformation of planar I* to a charge-transfer state (twisted or not) in either the nematic or melt phase of I-57 at the temperatures examined. Excitation at 360 nm *does* generate a polar species, interpreted here to be an excited charge-transfer state of I, A*, which suffers subsequent solvent relaxation manifested as a time-dependent Stokes shift.

Since the overall photophysical properties of I-57 in its nematic and melt phases are qualitatively similar, liquid-crystalline order may not play a dominant role in determining the rates of individual decay routes available to I* and its excited-state complexes.

Mechanistic Considerations

Excitation delocalization (or energy transfer and migration) can complicate the mechanistic schemes necessary to describe excimer/exciplex formation kinetics in liquid-crystalline media. When localization of the excitation energy at a particular

(43) Rettig, W. *J. Phys. Chem.* **1982**, *86*, 1970.

"chromophore" persists for a sufficiently long time, the rate of excimer formation is limited by the rate at which different liquid-crystalline orientations can be sampled. The distribution of the centers of mass of molecules in a liquid crystal is dictated by the type of mesophase and the molecular nature of the mesogen; a nematic phase like that formed by I-57 is translationally disordered (no center-of-mass correlation between molecules).[44] The presence of ground-state aggregates in concentrated hexane solutions of I suggests that even greater aggregation should be found in the neat nematic and melt phases of I-57. Indeed, the ~380 nm band attributed to fluorescence by excited monomers is nearly absent from the emission spectra of nematic I-57 and appears only as a weak shoulder in the melt phase. Thus, spatial molecular correlations which may exist in the nematic and melt phases of I-57 are imposed by intermolecular (pair) interactions.

Since the "excimer" notation implies a dynamically forming species with a dissociative ground state,[41,42] care must be exercised when dealing with systems where ground-state associations closely resemble the excited state configurations of the "excimer", as may be the case in neat phases of I-57. Stationary state spectra indicate that the 420 nm emission band, whose intensity is somewhat protracted in its time evolution, does not originate from the I* responsible for the band at ~380 nm. Furthermore, the presence of an "instantaneous" as well as a delayed emission component at 460 nm indicates that both dynamic and static processes contribute to the formation of the species responsible for the "excimer" I_{2b}*. Since a second complex, I_{2a}*, (leading to emission at 420 nm) has no component which is formed after excitation (i.e., after ca. 75 ps), the ground state of I-57 appears to consist primarily of two different complexes and some monomeric I.

The species emitting at 420 nm may be a dipole–dipole-stabilized antiparallel dimer in which cyano group-dipoles strongly interact.[45] Although it is tempting to assign the complex emitting at 460 nm to a dipole–dipole-stabilized dimer in which cyanophenyl groups completely (or nearly completely) overlap (as has been observed in the smectic and crystalline phases of 4′-alkyl- or 4′-alkoxy-substituted cyanobiphenyls,[46–50] and trans-1-alkyl-4-(*p*-cyanophenyl)cyclohexanes[51]), lack of a such a dimer in crystalline I with butyl, pentyl, hexyl, or octyl chains[45] raises doubts about its importance in I-57. However, it is conceivable that such a species can still exist in the more fluid nematic and melt phases of I-57. In fact, Markovitsi et al.[18a] have attributed two overlapping emission bands from cyanobiphenyl liquid crystals to a head-to-head and a head-to-tail excimer.

Although the model proposed here is consistent with our static and dynamic emission data, it is not unique. For instance, we cannot eliminate the possibility that some energy transfer occurs from I* to I_{2b} aggregates. This process can be described by a two state model in which a single exponential decay is predicted for the donor (I*) emission and a growth and a decay are predicted for emission from the acceptor (I_{2b}). In this case, the third component in the decay excited at 325 nm (and monitored at <450 nm) would be attributed to I_{2b}*, and the state yielding the 460 nm emission band would result from either directly excited ground-state dimers (or higher aggregates) or excimer-forming sites which act as traps for the initially produced excited state monomer. However, the fact that the emission bands at 380 and 460 nm can be observed selectively in concentrated hexane solutions of I indicates that this type of energy transfer is not an important process in I-57; we prefer the model in Scheme 2.

The time-dependent Stokes shift of the emission spectrum from I-57 excited at 360 nm is consistent with the instantaneous formation of a polar excited-state A* followed by solvent relaxation about it; "polar" here is synonymous with charge transfer. However, the nature and origin of the charge-transfer species, other than being monomeric, cannot be discerned from this work. Twisting of I* may be involved, but it need not be invoked to satisfy the kinetic scheme.

Theoretical treatments of time-dependent Stokes shifts[52] view the solvent as a continuum and the solute as a sphere of radius r and dipole moment μ_0. The interaction energy of the solute and its surroundings are described in terms of a reaction field and the solute parameters. According to the continuum model, the surrounding solvent molecules relax with a time constant τ_L, a characteristic, collective response of many solvent molecules, rather than a single molecular property like τ_D' (where $\tau_L = (\epsilon_\infty/\epsilon_0)\tau_D' \ll \tau_D'$ and τ_L and τ_D' are the longitudinal and Debye relaxation times, respectively). However, near a solute molecule in I-57, solvation is a result of reorganization of individual "solvent molecules" of I and should take place in a time scale closer to τ_D' than to τ_L.[53] Thus, the overall relaxation process should occur on several time scales in the range between τ_L and τ_D. For example, Maroncelli and Fleming[54] observed deviations from the continuum model for the picosecond solvation dynamics of a variety of alcohols, propylene carbonate, and *N*-methylpropionamide (using coumarin 153 as a probe molecule) and emphasized the importance of molecular aspects of the solvent.

A mean spherical approximation (MSA) treatment of dipolar hard-sphere solvent molecules has recently been proposed by Wolynes[55] and treated theoretically by Rips, Klafter, and Jortner.[56] However, while the MSA model predictions show the same behavior as the experimental spectral shift correlation function $C(t) = \{\nu(t) - \nu(\infty)\}/\{\nu(0) - \nu(\infty)\}$ (where $\nu(0)$, $\nu(t)$, and $\nu(\infty)$ are the average frequencies of the spectrum observed at times = 0, t, and ∞) and the same trend of the average time constant, quantitative agreement is rather poor.[53b] Furthermore, bias in the "solvent" molecular organization around the solute (for example, in liquid-crystalline environments) should require different time scales along different molecular axes.

Although we do not have dielectric data for I-57, its relaxation rate should be much slower and more complex than that of "ordinary" solvents near room temperature. In fact, dielectric relaxation studies[57] on *n*-alkylcyanobiphenyl liquid crystals, which have somewhat similar structures to our I molecules, reveal two relaxation processes in the direction parallel to the molecular director (10–20 ns and 1–2 ns) and one perpendicular to it (ca. 200 ps) in the nematic phases, and two relaxation processes (1–3 ns and ca. 100 ps) in the melt phases.[57] A fourth relaxation time, whose magnitude was not reported, was attributed to localized, ordered regions existing only in certain homologues. In those cases, the local order of the mesophase is retained partially in the isotropic phase, as witnessed by the persistence of three relaxation processes. Relaxation dispersion of nematic *trans*-4-(*p*-cyanophenyl)-*n*-heptylcyclohexane by the fast field-cycling NMR

(44) Vertogen, G.; de Jeu, W. H. *Thermotropic Liquid Crystals, Fundamentals*; Springer Series in Chemical Physics, Vol. 45; Springer-Verlag: Berlin, 1988.
(45) Sheikh-Ali, B. M.; Rapta, M.; Jameson, G. B.; Cui, C.; Weiss, R. G. *J. Phys. Chem.*, submitted.
(46) Leadbetter, A. J. In *Molecular Physics of Liquid Crystals*; Luckhurst, G. R., Gray, G. W., Eds.; Academic: New York, 1979.
(47) Cladis, P. E. Guillon, D.; Bouchet, F. R.; Finn, P. L. *Phys. Rev.* **1981**, *23A*, 2594.
(48) Longa, L.; de Jeu, W. H. *Phys. Rev. A* **1982**, *26*, 1632.
(49) Brownsey, G. J.; Leadbetter, A. J. *Phys. Rev. Lett.* **1980**, *44*, 1608.
(50) For instance, see: (a) Haase, W.; Paulus, H.; Müller, H. T. *Mol. Cryst. Liq. Cryst.* **1983**, *97*, 131. (b) Walz, L.; Paulus, H.; Haase, W. *Zeit. Kristall.* **1987**, *180*, 97.
(51) (a) Paulus, H.; Haase, W. *Mol. Cryst. Liq. Cryst.* **1983**, *92*, 237. (b) Furmanova, N. G.; Timofeeva, T. V. *Sov. Phys. Crystallogr.* **1986**, *31*, 601.
(52) (a) Bagchi, B.; Oxtoby, D. W.; Fleming, G. R. *Chem. Phys.* 1984, *86*, 257. (b) van der Zwan, G.; Hynes, J. T. *J. Phys. Chem.* **1985**, *89*, 4181.
(53) (a) Moroncelli, M.; Castner, E. W.; Webb, S. P.; Fleming, G. R. In *Ultrafast Phenomena V*; Fleming, G. R., Siegman, A. E., Eds.; Springer: Berlin, 1986; p 303. (b) Kahlow, M. A.; Kang, T. J.; Barbara, P. F. *J. Chem. Phys.* **1988**, *88*, 2372.
(54) Moroncelli, M.; Fleming, G. R. *J. Chem Phys.* **1988**, *89*, 875.
(55) Wolynes, P. G. *J. Chem. Phys.* **1987**, *86*, 5133.
(56) Rips, I.; Klafter, J.; Jortner, J. *J. Chem. Phys.* **1988**, *88*, 3246.
(57) Buka, A.; Owen, P. G.; Price, A. H. *Mol. Cryst. Liq. Cryst.* **1979**, *51*, 273.

technique[58] gave evidence for two relaxation processes of 1 and 5 ns, limited by the available frequency ranges.

According to the stationary-state and time-resolved fluorescence spectra of I-57, the species excited at 325 nm and 360 nm do not equilibrate completely, if at all, during their excited-state lifetimes. If the charge-transfer species is of the TICT-type, it must emanate from conformations which yield directly the charge transfer state (within the instrument resolution time of 75 ps).

Conclusions

The preferred model for excited state dynamics of I-57 which emerges from this data is very complex. The observation of (at least) two nonequilibrated excited-state complexes whose precursors are preformed in the ground state, and two monomeric excited states, which are clearly very different in their polarity and dynamic behavior, are curious and somewhat unexpected. However, even though the complicated kinetic model proposed in Scheme 2 is still overly simplified, it provides a reasonable basis for a tractable analysis; our assignments of structures to each of the species are somewhat nebulous, but they provide the most detailed insights to date into the interplay between molecular packing and electronic interactions[14,45] in systems with very high concentrations of molecules capable of forming ICT states. We are exploring further this interplay by examining the photophysical characteristics of the different homologues of I in their crystalline phases.[14,45]

Appendix

At a time t, after excitation by a delta-function of light, and assuming *no* equilibration between $\mathbf{I}^*$ and $\mathbf{I}_{2a}^*$, the rate equations for the model in Scheme 2 are presented in equations A1–A3.

$$\frac{d[I^*]}{dt} = k_{-1}[I^*_{2b}] - (k_2 + k_3 + k_1[I])[I^*] \quad (A1)$$

$$\frac{d[I^*_{2a}]}{dt} = -(k_6 + k_7)[I^*_{2a}] \quad (A2)$$

$$\frac{d[I^*_{2b}]}{dt} = k_1[I][I^*] - (k_4 + k_5)[I^*_{2b}] \quad (A3)$$

Solution to equation A2 is a single exponential decay function (eq A4).

$$[I^*_{2a}] = [I^*_{2a}]_o \exp\{-(k_6 + k_7)t\} \quad (A4)$$

Combining eqs A1 and A3 results in a second-order differential equation with the following solution:

$$[I^*] = \frac{1}{\Lambda_2 - \Lambda_1}\{\alpha_1 \exp(-\Lambda_1 t) + \alpha_2 \exp(-\Lambda_2 t)\} \quad (A5)$$

$$[I^*_{2b}] = \frac{1}{\Lambda_2 - \Lambda_1}\{\alpha_3 \exp(-\Lambda_1 t) + \alpha_4 \exp(-\Lambda_2 t)\} \quad (A6)$$

Where

$$2\Lambda_{1,2} = (X + Y) \pm \{(X - Y)^2 + 4k_1k_{-1}[I]\}^{1/2} \quad (A7)$$

$$\alpha_1 = k_{-1}[I^*_{2b}]_o - (X - \Lambda_2)[I^*]_o \quad (A8)$$

$$\alpha_2 = (X - \Lambda_1)[I^*]_o - k_{-1}[I^*_{2b}]_o \quad (A9)$$

$$\alpha_3 = (\Lambda_2 - Y)[I^*_{2b}]_o + k_1[I][I^*]_o \quad (A10)$$

$$\alpha_4 = (Y - \Lambda_1)[I^*_{2b}]_o - k_1[I][I^*]_o \quad (A11)$$

$X = k_1[I] + k_2 + k_3$ and $Y = k_{-1} + k_4 + k_5$. $[I^*]_o$, $[I_{2a}^*]_o$, and $[I_{2b}^*]_o$ are the concentrations of I^*, I_{2a}^*, and I_{2b}^* at $t = 0$.

Acknowledgment. The National Science Foundation (CHE-9213622) is gratefully acknowledged for its support of this research. We thank Dr. Jeff Byers, Dr. Dimirta Markovitsi, and Dr. Joseph Klafter for useful discussions during the course of this work. Drs. Scott A. Williams and C. Mark Phillips of the Regional Laser and Biotechnology Laboratories, University of Pennsylvania, are thanked for their help in performing the single photon counting experiments.

Supplementary Material Available: Four composite figures showing the fluorescence decay curves obtained from I-57 in its nematic (15 °C) and melt (25 °C) phases upon excitation at 325 or 360 nm and four tables of the associated decay constants and amplitudes (with χ^2 and Durbin–Watson parameters) (9 pages). This material is contained in libraries on microfiche, immediately follows this article in the microfilm version of the journal, and can be ordered from the ACS; see any current masthead page for ordering information.

(58) Noack, F.; Notter, M.; Weiss, W. *Liq. Cryst.* **1988**, *3*, 907.